

Received 24 July 2023; Accepted 31 October 2023
<https://doi.org/10.22226/2410-3535-2023-4-377-381>



On local lattice instabilities and polymorphism in the $\text{ZnS}_x\text{Se}_{1-x}:\text{M}$ ($M = 3d\text{-ions}$) sphalerite bulk crystals from neutron scattering

V. I. Maksimov[†], T. P. Surkova, E. N. Maksimova, V. D. Parkhomenko

[†]maximov@imp.uran.ru

Institute of Metal Physics, the UB RAS, Yekaterinburg, 620108, Russia

Abstract: The structure of solid solutions, or quasi-binary compounds, cubic $\text{ZnS}_x\text{Se}_{1-x}$ single crystals doped by $3d$ -ions M ($M = \text{V, Cr, Fe, Ni}$; M content was equal to 0.001; $0 \leq x \leq 1$) was investigated by thermal neutron diffraction. The revealed diffuse scattering effects illustrate the pronounced interplay between two the strongest destabilizing influences, which can coexist in the sphalerite crystal structure of II–VI compounds diluted by magnetic $3d$ -ions. Disturbance of the host crystal lattice going from doped Jahn-Teller $3d$ -ions leading to a tendency to form superstructures. The structure instabilities of the solid solution matrices came from high degree polymorphism being especially intrinsic for ZnS, can result in anomalous enlarging of shear atomic displacement amplitudes along the directions of minimum of interatomic distances corresponding to the $\langle 110 \rangle$ crystallographic directions.

Keywords: diluted magnetic semiconductors (DMS), single crystals, neutron diffraction, crystal structure

1. Introduction

Over the past two decades there has been considerable interest in the study of II–VI semiconductor compounds doped with $3d$ -ions (V^{2+} , Cr^{2+} , Mn^{2+} , Fe^{2+} , Co^{2+} , Ni^{2+}). These materials belong to the class of dilute magnetic semiconductors (DMS), which are mainly associated with the construction of Zn-chalcogen-based lasers [1–2] and the attempts to create electronic devices with spin-polarized currents (spintronics) [3–4]. Some important and significant results of the DMS-study were obtained on nanoscale samples of such materials in the last decade [5–9]. One remarkable property of the materials of this type is that some of them can form quasi binary systems with each other (via cationic and/or anionic substitution) [10,11]; the $\text{ZnS}_x\text{Se}_{1-x}$ system belongs to this type of solid solutions [10]. One of the attractive aspects of studying the physical properties of such compounds is to understand effectiveness to achieve apparent possibilities in driving crystal and band structure parameters. However, it was shown by EXAFS and simulations [12,13 and refs therein] that the local atomic order of such alloys having sphalerite structure undergoes some distortion disordering. A real crystal structure of such compounds can be represented by presence of strained atomic tetrahedrons distributed within crystal lattice with respect to bulk volume, because S and Se anions composing quasi binary zinc-chalcogen solid solutions determine two slightly different parameters of chemical bond length in pure ZnS and ZnSe compounds [11]. Previously, thermal neutron diffraction study showed [13–16] that magnetically active $3d$ -ions doped onto ZnSe matrix induce strong destabilization influence on the host crystal lattice. It has been revealed two types of local cubic lattice distortions in a wide temperature range, namely, nanodeformations of the

trigonal type tendency caused by Ni and V ions and distortions of the tetragonal type induced by Cr and Fe ions. The local distorted lattice regions were considered to be rather long (about 10 nm) in comparison with the unit-cell parameters of the initial compound. As to sphalerite crystal structure within full sequence zinc-chalcogen compounds is concerned, tendencies to polytypes forming seems another destabilizing problem, with ZnS being the most known material to undergo the such disordering influence. Quasi homogeneous solid solutions $\text{ZnS}_x\text{Se}_{1-x}$, as to x changes, also can be highly sensitive to preferences of atomic layers stacking to choose sequences with tending to stability, which have been shown in [17]. Therefore, there are several different destabilizing influences based on sphalerite of II–VI compounds, which could give resulting interplay in the crystal structure whenever $\text{ZnS}_x\text{Se}_{1-x}$ crystals being doped by magnetically active $3d$ -impurities. With long range ferromagnetic order being the most interesting search subject for investigations performed on II–VI DMS today [3–4], noting that the establishment of any magnetic ordering is not only function of magnetically active ions content in non-magnetic semiconductor matrix but it may depend on ordering character between magnetic ions in the host crystal lattice. Taking into account additional degree of the $\text{ZnS}_x\text{Se}_{1-x}$ lattice degradation constructed by the anion substitution at specified x variables, the main goal of our work was to investigate possible tendencies to atomic and distortion regulating which could be considered as a favorable factor to solute $3d$ -impurities onto II–VI matrix and to establish any magnetic ordering. In this paper we report the results, having studied by neutronography, of fine features of the crystal structure of cubic compounds $\text{Zn}_{0.999}\text{M}_{0.001}\text{S}_x\text{Se}_{1-x}$ ($M = \text{V, Cr, Fe, Ni}$; $x = 0, 0.1, 0.2, 0.3, 0.4, 0.5, 0.6, 0.7, 0.8, 1.0$), obtained by vapor phase chemical transport.

2. Materials and experimental methods

2.1. Samples

All samples grown by the vapor transport technique (by V. Girit, A. Lopez, Universidad de los Andes, 5101 Merida, Venezuela) were of a non-regular geometrical shape. The approved and carefully-controlled technique of crystal-growth serves as guarantee the precision of the substitution and dopant-amount given in chemical formulas of the crystals. The average linear size of $Zn_{0.999}M_{0.001}S_xSe_{1-x}$ single crystal samples did not exceed 5×10^{-3} m. The plane faces (chips) of the crystals corresponding to (110), (100) or, rarely, (111) crystallographic planes. Both the relative simplicity of the crystal structure of the compounds, and high intensity of the main Bragg peaks make easy adjustment of single crystals for executing neutron diffraction experiments.

2.2. Experiment

Our neutron diffraction experiments on elastic thermal neutron scattering have been performed on the D7b multichannel two-axis single crystal diffractometer at the IVV-2M research reactor (Sverdlovsk region, Zarechny, Russia) [18]. The incident neutron wavelength was $\lambda = 1.57$ Å; the neutron beam was formed by a double monochromator crystal system composed of pyrolytic graphite and germanium. The angular instrumental error of our diffractometer equals 0.0056° determined (checked by the calibration of the diffractometer) from metrology tests. The error of pulse count is taken from the well-known equation: $\sigma_N = \sqrt{N}$, where σ_N is the absolute error, N is the pulse count.

3. Results and discussion

The strongest Bragg reflections of all crystals were carefully checked by ω -scans and a number of non-perfect crystals have been rejected for neutronographic experiment. As it can be understood from [17], that the ZnS_xSe_{1-x} compounds are very "capricious" to synthesize them in strictly definite modification of their crystal structure. Unfortunately, the poorest crystals were those contained V and Ni doped ions, but the information obtained have been enough to represent the common picture of fine crystal structure features having place in the sphalerite modification of the ZnS_xSe_{1-x} solid solutions bulk crystals doped by $3d$ -ions. Despite the indications on non-small crystal blocks presence being sometimes visible, at least a large massive perfect single crystal fragment to be the most suitable for neutron diffraction experiment exists in each crystal sample having been chosen for our neutronography research. These results of ω -scans show the only reflections scanned, with peaks having symmetrical forms (well-described by Gaussian profile) and their halfwidths being near $0.10 - 0.15^\circ$ in visible diffractometer optical diapason. The best and the most clear results have been obtained on $ZnS_{1-x}Se_x:M$ ($M = Cr, Fe$) samples.

Our neutron diffraction experiment confirms that the main structural motif of $ZnS_{1-x}Se_x:M$ compounds grown

by chemical transport corresponds to the fcc lattice. The dependence $a(x)$ of lattice parameter is linear within the measurement error, with the conclusion allowed its character to be corresponded to Vegard's law.

The main information about structure inhomogeneities formed in the crystal lattice of the II-VI crystals can be obtained from the diffuse scattering effects appearing near Bragg reflections. One can find some data about inhomogeneous deformations of based on II-VI DMS's fcc lattice, caused by Jahn-Teller $3d$ -ions, in [13-16], where the most part of neutronographic results associated mainly with transverse directions have been discussed in detail. The detailed descriptions of neutron diffuse scattering effect analysis performed for diffraction pictures obtained on II-VI compounds diluted by $3d$ -ions can be found in [13].

The picture of fine diffraction effects related to the chemical compositions of $ZnS_{1-x}Se_x:M$ compounds is rather interesting. As it had been shown in [13-16], $3d$ -ions doped into II-VI bulk material can induce inhomogeneous nanoscale regions increasing on cooling and two clear topologies of distorted regions (with the marked effect being the most visible at lower temperatures, depending on $3d$ -configurations) can be highlighted. Trigonal type on V, Ni ions inserted (for which the maximal L values correspond to $\langle 100 \rangle$ and $\langle 011 \rangle$ directions at $T = 78$ K), and tetragonal type when Cr, Fe ions incorporated in the host matrix (the $\langle 1-10 \rangle$ direction characterized by the largest elongation of nanodistorted regions at $T = 78$ K). The L results obtained by the present work on $ZnS_{1-x}Se_x:M$ crystals show qualitatively analogous behavior of correlation lengths L vs sort of $3d$ -ion doped into ZnS_xSe_{1-x} matrixes. Moreover, L values for all $ZnS_xSe_{1-x}:Fe$ samples seems to be the same as for $ZnSe:Fe$, while L for $ZnS_xSe_{1-x}:Cr$ series slightly differ in quantities on different x without any regularity (Table 1).

Neutron diffraction scans of $\{220\}$ type reflections of $ZnS:M$ ($M = Fe, Cr$) measured in longitudinal direction reveal a systematic modulations of backgrounds while these type of scans obtained on crystals characterized by substitution amount x differed from 1 and up to 0 value did not show any anomalies like those presented by Fig. 1 (here and further the symbol size corresponds the error of pulse count, the error determined by the angular resolution is less than the symbol size over all the graphs on the presented scales).

These weak superstructure maxima (Fig. 1) well correspond to the $q = (1/3, -1/3, 0)2\pi/a$ (a — parameter of the cubic crystal lattice). Observed result suggests about quasi-periodical longitudinal shifts of crystal lattice ions in planes having minimal distances between one-type ions. As it have been discussed for $ZnS:Fe$ crystal elsewhere [19] in

Table 1. Values of correlation lengths L (nm) in the symmetric crystallographic directions for $ZnS_xSe_{1-x}:Cr$ crystals.

x in $ZnS_xSe_{1-x}:Cr$ composition	(Reflection)[direction]					
	(220)[1-10]		(022)[100]		(400)[011]	
	300 K	78 K	300 K	78 K	300 K	78 K
0	12.0	>60	12.0	(16 ± 2)	4.0	(10 ± 2)
0.2	13.5	>60	11.0	(17 ± 2)	5.0	(10 ± 2)
0.5	9.5	>60	10.5	(15 ± 2)	8.0	(11 ± 2)
0.7	10.5	>60	11.5	(16 ± 2)	9.0	(11 ± 2)

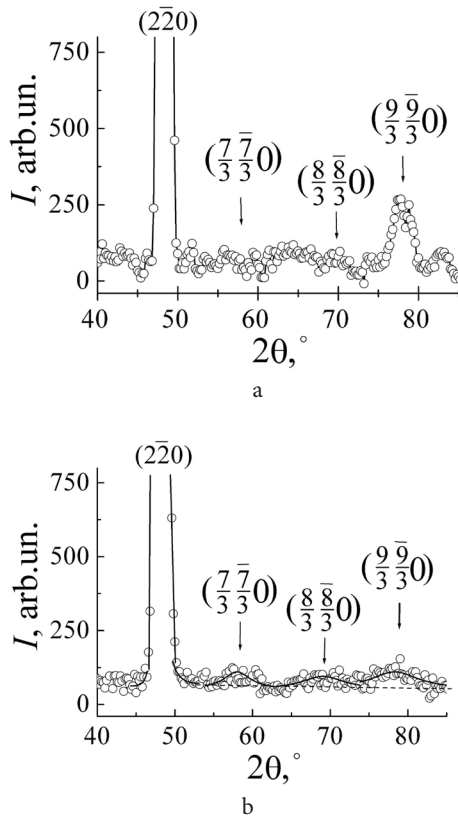


Fig. 1. Neutron diffraction scans measured at $T=300$ K along straight-line trajectory through (2-20) knot for $\text{ZnS}:M$, $M=\text{Cr}$ (a); $M=\text{Fe}$ (b) single crystals in [1-10] direction.

more details, revealed instability of the crystal lattice can be based on ability to polytypism of pure ZnS. At small amount of doped 3d-ions ZnS can retain a tendency to form one of the most its typical polytype having 6H-structure.

In the present work neutronographic data obtained on $\text{ZnS}_x\text{Se}_{1-x}:M$ single crystals reveal diffuse scattering effects associated with interplay between two the strongest destabilizing influences which can coexist in the sphalerite crystal structure of DMS. The Fig. 2 shows an example of substitution degree dependencies of diffuse maxima for $\text{ZnS}_x\text{Se}_{1-x}:M$ ($M=\text{Fe}, \text{Cr}$) series. At first, the intensity of the diffuse contributions for $\text{ZnS}_x\text{Se}_{1-x}:M$ near {220}-type reflections measured along [1-10] (and so, [11-2], not shown) directions decreases as x increases, which may reflect a behavior of destabilizing tendency going from Jahn-Teller 3d-ions doped in the host crystal lattice. This fact is in agreement with our suggestion about heightened sensitivity of the crystal lattice to form shear strains at increasing element periodic system number of chalcogen belonging to the matrix compound [20]. The Fig. 3 illustrates our neutron diffraction data measured near (400) reflection along [011] direction. As the selenium content decreases in $\text{ZnS}_x\text{Se}_{1-x}$, it can result in anomalous enlarging of shear atomic displacement amplitudes in {110} directions characterized by the minimum of interatomic distance.

The {110} crystallographic directions are the ones in which instability conditioned by polytypism is observed. The described results obtained by neutronography, to compare with the literature data, indicate on the non-simplicity of local

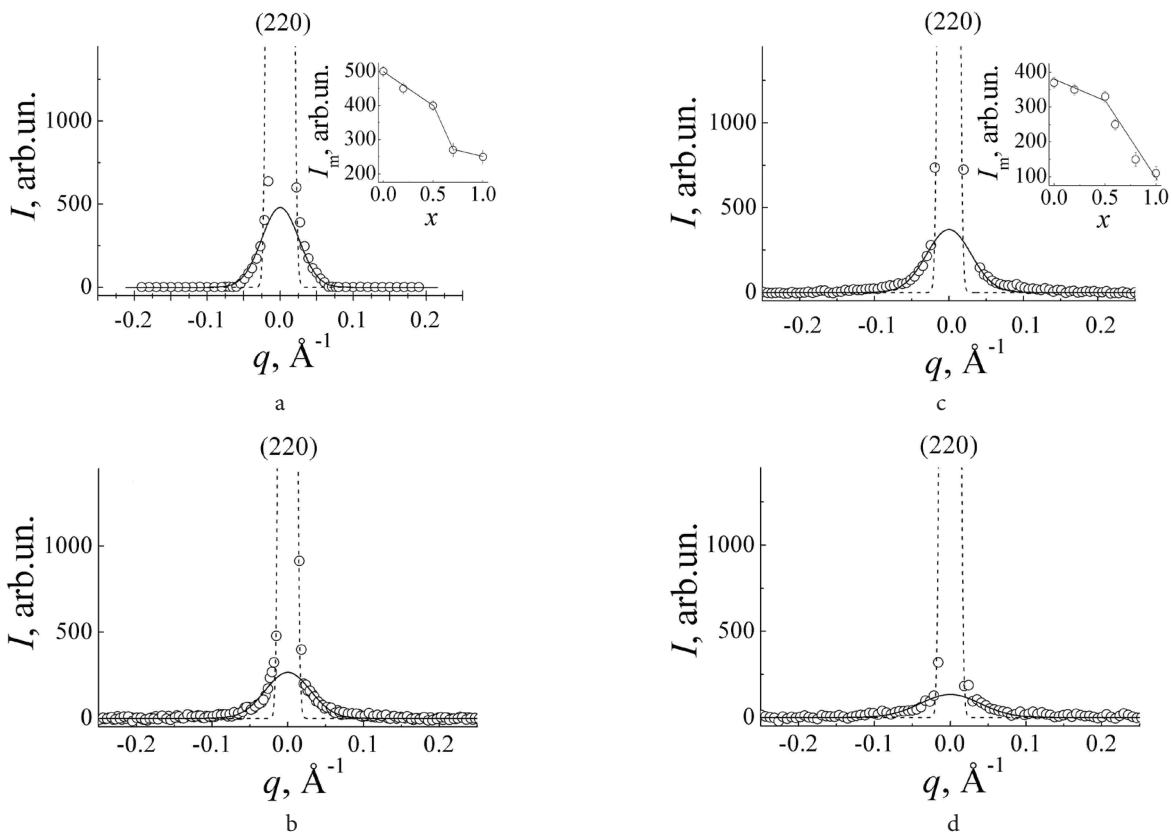


Fig. 2. Neutron diffraction scans of (220) reflection measured along [1-10] direction at $T=300$ K for $\text{ZnS}_x\text{Se}_{1-x}:\text{Cr}$, $x=0$ (a), $x=0.7$ (b) and $\text{ZnS}_x\text{Se}_{1-x}:\text{Fe}$, $x=0$ (c), $x=0.8$ (d) single crystals. \circ — experimental results; dash lines — Gauss profiles of Bragg peaks; solid lines — diffuse contributions of reflections. Insets illustrate substitution-dependencies of diffuse maxima values for $\text{ZnS}_x\text{Se}_{1-x}:\text{Cr}$ (a) and $\text{ZnS}_x\text{Se}_{1-x}:\text{Fe}$ (c) systems.

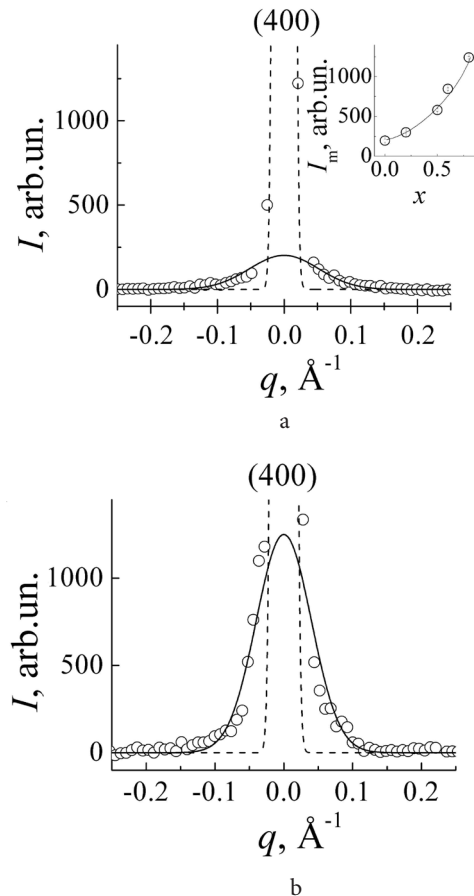


Fig. 3. Neutron diffraction scans of (400) reflection measured along [011] direction at $T=300$ K for $\text{ZnS}_x\text{Se}_{1-x}:\text{Fe}$ $x=0$ (a), $x=0.8$ (b) single crystals. \circ — experimental results; dash lines — Gauss profiles of Bragg peaks; solid lines — diffuse contributions of reflections. The inset illustrates substitution-dependence of diffuse maxima values.

crystal structure states existed in sphalerite modification of $3d$ -ions-DMS based on $\text{ZnS}_x\text{Se}_{1-x}$ solid solutions. So that the investigated compounds have been doped by small amount of $3d$ -ions, another interesting effects, which are possible to observe by single crystals neutronography — such as self-organization of doped ions and/or shear atomic displacements regions in the sphalerite crystal lattice of II–VI crystals — could not be considered. To obtain more information about possibilities for synthesis DMS based on II–VI compounds and their solid solutions for spintronic applications, it needs to obtain single crystals with a doping level of $3d$ -ions close to solubility limit, and to perform combined neutronographic and magnetic measurements.

4. Conclusions

The results of neutron diffraction research of fcc $\text{Zn}_{0.999}\text{M}_{0.001}\text{S}_x\text{Se}_{1-x}$ single crystals ($M=\text{V}, \text{Cr}, \text{Fe}, \text{Ni}$; $0 \leq x \leq 1.0$) obtained by vapor phase chemical transport were discussed. A *priori* degradation of the $\text{ZnS}_x\text{Se}_{1-x}$ sphalerite crystal lattice does not seem to be visible by neutronography and to play essential role in forming any tendencies to structural orderings at small dopant content. The scattering effects, which are caused by transverse and longitudinal

local deformations, are indicative of two coexisting types of lattice instability for these crystals. The local deformations caused by these instabilities depend strongly on the crystal composition. When sulfur dominates, nanodeformations are basically related to the lattice tendency to form polytypes, while the instability effects caused by the incorporation of $3d$ -ions are less pronounced. The effects of longitudinal deformations have been observed to be the most pronounced in $\text{Zn}_{0.999}\text{M}_{0.001}\text{S}$ crystals along the {011} directions (corresponding to the closest ion packing) in the fcc lattice. The period of these deformations is described by the wave vector $q = n(1/3, -1/3, 0)2\pi/a$, ($n=1, 2, 3$).

Acknowledgements: The results of the present work were obtained at IMP Neutron Material Science Complex within the state assignment of Ministry of Science and Higher Education of the Russian Federation (themes “FLUX” No. 122021000031-8, “ELECTRON” No. 122021000039-4).

References

1. V.Yu. Ivanov, M. Godlewski, T.P. Surkova, N. Zhavoronkov, A.R. Omelchuk. Phys.Stat.Sol. (b). 229, 355 (2002). [Crossref](#)
2. S.B. Mirov, I.S. Moskalev, S. Vasilyev, V. Smolski, V.V. Fedorov, D. Martyshkin, J. Peppers, M. Mirov, A. Dergachev, V. Gapontsev. IEEE Journal of Selected Topics in Quantum Electronics. 24, 1601829 (2018). [Crossref](#)
3. T. Dietl. Nature Materials. 9, 965 (2010). [Crossref](#)
4. J.M. Baruah, J. Narayan. Dilute Magnetic Semiconducting Quantum Dots: Smart Materials for Spintronics. In: Nonmagnetic and Magnetic Quantum Dots (ed. by V.N. Stavrou). IntechOpen (2018) 187 p. [Crossref](#)
5. H. Wang, J. Gao, M. Zhang, P. Liu, Y. Guo, H. Li, G. Zhao, S. Hu, Z. Cheng, J. Zang, R. Wen, T. Liu, Yu. Tong, Z. Sun, H. Wang. ACS Appl. Nano Mater. 5, 8448 (2022). [Crossref](#)
6. A. C. A. Silva, A. I. S. Barbosa, A. S. Silva, E. A. Batista, T. K. de Lima Rezende, É. V. Guimarães, R. S. Silva, Noelio O. Dantas. In: Materials at the Nanoscale (ed. by A. Mallik). IntechOpen, E-book (2021) 339 p. [Crossref](#)
7. P. Zhang. Magneto-optical Studies of Mn Doped II–VI Group Semiconductor Nanostructures: PhD thesis. The State University of New York (2019) 243 p.
8. M.T. Pham, N.X. Ca, P.N. Loan, N. Tran, B.T. Huy, N. T. Dang, T.L. Phan. J. Supercond. Nov. Magn. 32, 1761 (2019). [Crossref](#)
9. A. Rafiq, M. Imran, M. Aqeel, M. Ikram, H. Majeed, S.G. Hussain, S. Ali. Nanosci. and Nanotech. Lett. 11, 1060 (2019). [Crossref](#)
10. S.S. Gorelik, M.Ya. Dashevskii. Materials Science of Semiconductors and Insulators. MISIS, Moscow (2003) 480 p. (in Russian)
11. B.V. Robouch, E. Burattini, A. Kiseil, J. Konior, A.L. Suvorov, A.G. Zaluzhnyi. In: Modern Condensed Matter Physics: Experimental Methods and Devices, Related topics: proceedings of the 4th Moscow International ITEP School of Physics. Moscow,

- Akademprint (2001) pp. 113–126.
12. Semimagnetic Semiconductors (ed. by J. Furduna and J. Kosuta). Mir, Moscow (1992) 526 p. (in Russian)
 13. S.F. Dubinin, V.I. Sokolov, S.G. Teploukhov, V.D. Parkhomenko, N.B. Gruzdev. Phys. of the Solid State. 48, 2275 (2006). [Crossref](#)
 14. V.I. Maksimov, E.N. Maksimova, T.P. Surkova, A.P. Vokhmyanin. Phys. Solid State. 60, 2424 (2019). [Crossref](#)
 15. V.I. Maksimov, E.N. Maksimova, T.P. Surkova, V.D. Parkhomenko. J. Surf. Investigation. 14, 31 (2020). [Crossref](#)
 16. V.I. Maksimov, E.N. Maksimova, T.P. Surkova, V.D. Parkhomenko. Phys. Solid State. 63, 1212 (2021). [Crossref](#)
 17. E. Michalski, M. Demianiuk, S. Kaczmarek, J. Zmija. Acta Physica polonica A. 58, 711 (1980).
 18. B. Goshchitskii, A. Menshikov. Neutron News. 7, 12 (1996). [Crossref](#)
 19. V.I. Maksimov, S.F. Dubinin, T.P. Surkova, V.D. Parkhomenko. Phys. of the Solid State. 54, 1131 (2012). [Crossref](#)
 20. V.I. Maksimov, S.F. Dubinin, V.D. Parkhomenko. Crystallography reports. 56, 1169 (2011). [Crossref](#)